

Contoured-Beam Dual-Band Dual-Linear Polarized Reflectarray Design Using a Multi-Objective Multi-Stage Optimization

Daniel R. Prado, Manuel Arrebola, *Senior Member, IEEE*, Marcos R. Pino
and George Goussetis, *Senior Member, IEEE*

Abstract—This work presents a dual-band design procedure applied to a very large contoured-beam reflectarray with improved copolar and cross-polarization performances for direct broadcast satellite in dual-band dual-linear polarization. The reflectarray is elliptical, with axes of 1.10 and 1.08 meters, and provides coverage for South America in transmit (11.70 GHz–12.20 GHz) and receive (13.75 GHz–14.25 GHz) bands. The novel dual-band design approach is based on the use of a multi-resonant unit cell with several degrees of freedom (DoF). It is divided in several stages to facilitate convergence towards a broadband high-performance reflectarray. First, a narrowband layout is obtained at central frequency with a phase-only synthesis. Then, using a limited number of DoFs, a copolar-only optimization is carried out in both frequency bands maximizing the copolar figure of merit. Finally, increasing the number of DoF, cross-polarization requirements are also included in the optimization procedure. The optimized antenna complies with all copolar and cross-polarization requirements with a loss budget of at least 0.62 dB in both receive and transmit bands, outperforming earlier works in the literature while using a smaller antenna than previously proposed for this mission.

Index Terms—Broadband reflectarray, contoured-beam, optimization, transmit-receive antennas, DBS antennas, satellite antennas

I. INTRODUCTION

REFLECTARRAY antennas usually exhibit narrow bandwidth which is primarily the result of two factors: the low bandwidth of resonant elements and the differential spatial phase delay [1]. Several multi-resonant wideband elements have been proposed to tackle the first limitation, such as stacked patches, patches aperture-coupled to delay lines [1], parallel dipoles [2] or the Phoenix cell [3], among others. Bandwidth may also be improved by using an artificial impedance surface in the form of sub-wavelength elements. Several elements of this kind have been proposed [4]–[6], all of them applied to small-sized reflectarrays with collimated beams. However, they may present some limitations when employed in very large reflectarrays for contoured-beam applications, due to the fact that they do not provide a full 360° phase-shift [4]. This may limit the reflectarray performance and the antenna operation to a single polarization [5] while also pose computational challenges associated

This work was supported in part by the Ministerio de Ciencia, Innovación y Universidades under project TEC2017-86619-R (ARTEINE); by the Ministerio de Economía, Industria y Competitividad under project TEC2016-75103-C2-1-R (MYRADA); by the Gobierno del Principado de Asturias/FEDER under Project GRUPIN-IDI/2018/000191; by Ministerio de Educación, Cultura y Deporte / Programa de Movilidad “Salvador de Madariaga” (Ref. PRX18/00424).

D. R. Prado, M. Arrebola and M. R. Pino are with the Department of Electrical Engineering, Universidad de Oviedo, Gijón, Spain (e-mail: drprado@uniovi.es; arrebola@uniovi.es; mpino@uniovi.es).

G. Goussetis is with the Institute of Sensors, Signals and Systems, School of Engineering and Physical Sciences, Heriot-Watt University, Edinburgh, U.K. (email: g.goussetis@hw.ac.uk).

Color versions of one or more of the figures in this paper are available online at <http://ieeexplore.ieee.org>.

Digital Object Identifier XX.XXXX/LAWP.XXXX.XXXXXXXX

with the unit cell complexity [6]. For the latter problem there are several strategies that may be applied, such as optimizing the geometry of the unit cell at several frequencies [2], increasing the F/D ratio [1], using curved [7] or multi-faceted reflectarrays [8]. However, using curved or multifaceted reflectarrays complicates the antenna structure with regard to planar reflectarrays, while increasing the F/D ratio produces a larger antenna and increases spillover for a given feed, although the spillover efficiency could be solved using a more directive feed.

In addition, several techniques have been proposed for the crosspolar optimization of reflectarray antennas. Some techniques work at the element level and include a suitable arrangement of reflectarray elements to cancel cross-polarization effects [9], reduction of the undesired tangential field [10] and element rotation [11]. The element rotation technique has also been applied with success to polarizers to lower their cross-polarization [12]. A better approach, albeit computationally more expensive, is the direct optimization of reflectarray antennas [3], [13]–[16], where all reflectarray elements are optimized at the same time, providing improved results. This can be done using databases [13], [14], a full-wave technique based on local periodicity [15] or machine learning algorithms such as support vector machines [16] or artificial neural networks [3]. The reflectarrays considered in [15] and [16] were optimized only at a single frequency, and thus they operate in a narrow bandwidth. In [3] a reflectarray was optimized in a 16% bandwidth, but only considering single circular polarization with no cross-polarization requirements. In [13] a shaped-beam single-polarized reflectarray with European coverage was optimized in a 20% bandwidth. A similar reflectarray was later optimized in [14] considering dual-linear polarization and cross-polarization performance.

The previous broadband reflectarrays work in a single band. Transmit-receive contoured-beam reflectarrays have also been designed in [17]–[19], where a South American coverage was considered for transmit (11.70 GHz–12.20 GHz) and receive (13.75 GHz–14.25 GHz) bands. The reflectarray in [17] has a diameter of 1.2 meters and it is based on three stacked patches of varying size. The design procedure consisted in several stages of a phase-only synthesis, and copolar requirements were met in more than 90% of the coverage in both bands. However, cross-polarization requirements were not fully accomplished since they were not taken into account in the design procedure. The same reflectarray was later designed in [19] using a direct optimization procedure, fulfilling all coverage requirements with a loss budget of 0.4 dB. In this context, the loss budget is defined as a quantity to add on top of the minimum specifications to ensure that requirements are met since there may be losses in gain not taken into account in the analysis, such as manufacturing tolerances. In [18] the size of the reflectarray was reduced from 1.2 meters to 1.1 meters, achieving a similar performance as the reflectarray in [17] but with a smaller size. Also, [19] employed an ideal far field model

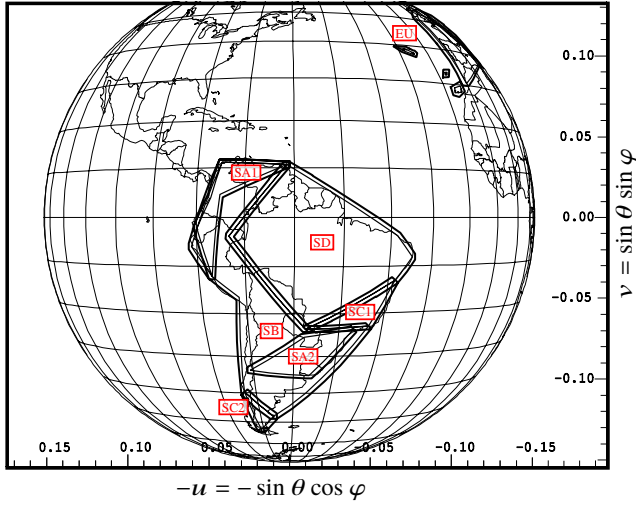


Fig. 1. South American coverage [17] (© 2011 IEEE).

for the feed to design the reflectarray.

In this work, we present a new dual-band design procedure based on a multi-resonant unit cell with up to eight degrees of freedom (DoF) and the generalized intersection approach (gIA). The gIA is improved to include a multi-objective and multi-frequency cost function; and the optimization of the copolar figure of merit, namely the minimum copolar gain for each coverage zone. In addition, the procedure is divided into several stages, gradually increasing the complexity of the problem and the total number of DoFs in order to facilitate convergence towards a dual-band design. The procedure is as follows. First, a narrowband design is obtained with a phase-only synthesis. Then, a copolar-only dual-band design is carried out with a limited number of DoFs, which are subsequently increased while including cross-polarization requirements as well. This guided optimization procedure assists in obtaining a dual-band high-performance reflectarray, which otherwise would be unattainable. It was applied to the design of a 1.10×1.08 -meters elliptical, transmit-receive reflectarray for space applications in Ku band with a South American coverage in dual-linear polarization with very tight copolar and crosspolar requirements. After the optimization, the reflectarray outperforms others reported in the literature, with a loss budget of at least 0.62 dB, while having a smaller aperture and considering the near field of a real feed horn.

The rest of the paper is organized as follows. Section II reviews the mission requirements and antenna optics. Section III describes the dual-band design and optimization procedure. Section IV presents the results of the reflectarray with South American coverage. Finally, Section V contains the conclusions.

II. MISSION REQUIREMENTS AND ANTENNA OPTICS

The same South American coverage as in [17]–[19] is considered. It corresponds to the PAN_S mission from the Amazonas spacecraft operated by Hispasat. The South American continent is divided into six different coverage zones as shown in Fig. 1, each one with the requirements gathered in Table I for the transmit and receive bands. In addition, it also includes copolar isolation for Europe, specifying a maximum gain of 0 dBi over that area. This mission operates in dual-linear polarization. In addition, the coverage shown in Fig. 1 includes a margin of 0.1° for the antenna pointing error in all axes (roll, pitch and yaw).

The real antenna used on board of the satellite for the PAN_S mission is a Gregorian dual-reflector antenna comprised of a 1.5-meter

Table I
REQUIREMENTS FOR THE SOUTH AMERICAN COVERAGE IN DUAL-LINEAR POLARIZATION FOR THE ZONES DEFINED IN FIG. 1. GAIN REFERS TO MINIMUM COPOLAR GAIN WITH THE EXCEPTION OF EU, WHICH IS MAXIMUM COPOLAR GAIN.

Zone	Tx (11.70 GHz–12.20 GHz)		Rx (13.75 GHz–14.25 GHz)	
	Gain (dBi)	XPD (dB)	Gain (dBi)	XPI (dB)
SA1	28.82	31.00	27.32	32.00
SA2	28.81	31.00	27.31	28.00
SB	25.81	30.00	24.31	28.00
SC1	22.81	29.00	22.31	28.00
SC2	20.66	27.00	21.28	28.00
SD	19.81	27.00	18.31	25.00
EU	0.00	—	0.00	—

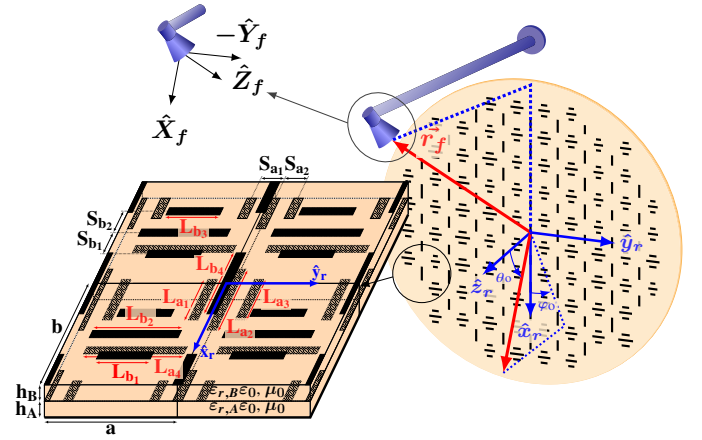


Fig. 2. Sketch of the reflectarray antenna geometry and unit cell based on two sets of parallel dipoles employed in this work [21] (© 2018 IEEE).

main shaped reflector and a 50-cm subreflector [17]. However, in this work a single-offset 1.1-meter flat reflectarray will be considered to fulfil the same requirements, in contrast to the reflectarrays designed in [17] and [19] that have a diameter of 1.2 meters. A sketch of the reflectarray optics is shown in Fig. 2. It is an elliptical reflectarray with axes of 1.10 and 1.08 meters, comprised of 7772 elements in a regular grid of 110×90 unit cells for polarization X, and 109×89 unit cells for polarization Y. The periodicity is $10 \times 12 \text{ mm}^2$. A circular corrugated horn is employed as feed. Its near field has been obtained using a spherical wave expansion with commercial software [20] at several frequencies and employed in the dual-band design procedure. This contrasts with previous works [19] that employ an ideal far field model in the design. The center of the horn aperture is placed at $\vec{r}_f = (-366, 0, 1451) \text{ mm}$ with regard to the reflectarray center and generates an illumination taper of -14 dB in the transmit band and -18 dB in the receive band.

III. DUAL-BAND DESIGN PROCEDURE FOR ELECTRICALLY LARGE REFLECTARRAYS

A. Brief Description of the Unit Cell

The same unit cell used in [15] and shown Fig. 2 is employed here. It is thoroughly described in [2], but it will be briefly reviewed here for completeness. It is based on two sets of parallel and coplanar dipoles in two layers of metallization. Each set of dipoles controls the phase-shift for a linear polarization, i.e., the dipoles oriented along the \hat{x}_r axis control the phase-shift for polarization X, and the dipoles oriented along the \hat{y}_r axis control the phase-shift for polarization Y. This unit cell has been designed to provide broadband behaviour,

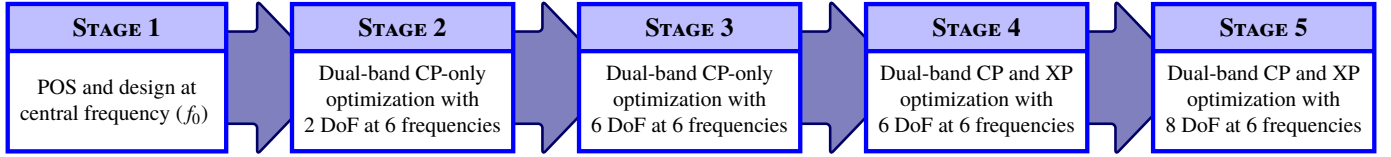


Fig. 3. Flowchart of the dual-band optimization procedure.

low losses, low cross-polarization and independent control of the phase-shift for two linear polarizations. The broadband behaviour is achieved by having multiple resonances, producing a linear and wide phase-shift range. A full-wave method of moments based on local periodicity [22] is employed for the cell analysis in the dual-band optimization procedure. It has been validated by means of full-wave simulations with commercial software [11] and prototypes [2].

The phase-shift is controlled by the length of the dipoles. Thus, this unit cell provides up to eight DoFs for optimization purposes, and they are shown in red in Fig. 2. The rest of the unit cell parameters will be fixed. In particular, their width is set to 0.5 mm while the separation center to center between them is set to 2.5 mm. Commercial substrates were chosen, the Arlon AD255C for layer A and the Diclad 880 for layer B.

B. Generalized Intersection Approach

The optimization procedure is based on the generalized intersection approach (gIA). A complete formulation of the analysis and optimization framework has been presented elsewhere for a monochromatic case [15], [23]. Here we introduce two novelties in the algorithm with regard to previous works: the extension of the algorithm to multi-frequency for dual-band optimization, along with a suitable optimization procedure to facilitate convergence towards a dual-band high-performance design; and the optimization of the figure of merit for the copolar pattern combined with a multi-objective optimization (minimum and/or maximum copolar gain, crosspolar discrimination and crosspolar isolation).

The optimization of the cross-polarization figures of merit was introduced in [21]. Following this methodology, instead of the usual approach of minimizing the crosspolar pattern, the crosspolar discrimination (XPD) or the crosspolar isolation (XPI) are maximized in the transmit and receive bands, respectively. This can be extended to consider the figure of merit for the copolar pattern. In the present case, the minimum copolar gain will be maximized in each coverage zone. Hence, if T is the minimum or maximum specification template, the following condition should be met in the forward projector:

$$T_{CP_{\min}} \leq CP_{\min}, \quad (1)$$

$$T_{CP_{\max}} \geq CP_{\max}, \quad (2)$$

where $CP_{\min/\max}$ is the minimum or maximum copolar gain defined for a coverage area and polarization. This allows to accelerate the algorithm and to reduce the memory footprint roughly by half.

To achieve broadband performance, the optimization will be carried out in several frequencies simultaneously. Thus, the cost function minimized in the backward projection [15] is modified as follows:

$$F = \sum_{f=1}^{N_f} \sum_{m=1}^M \left\{ W_{f,1}(\vec{r}_m) [CP'_{\min/\max,f}(\vec{r}_m) - CP_{\min/\max,f}(\vec{r}_m; \vec{\xi})] + W_{f,2}(\vec{r}_m) [XPD'_{\min,f}(\vec{r}_m) - XPD_{\min,f}(\vec{r}_m; \vec{\xi})] + W_{f,3}(\vec{r}_m) [XPI'_f(\vec{r}_m) - XPI_f(\vec{r}_m; \vec{\xi})]^2, \right. \quad (3)$$

where N_f is the number of frequencies at which the optimization is performed; M is the number of number of coverage zones; \vec{r}_m is an obser-

vation point in the coverage zone; $CP'_{\min/\max,f}(\vec{r}_m)$, $XPD'_{\min,f}(\vec{r}_m)$ and $XPI'_f(\vec{r}_m)$ are the reference parameters; $CP_{\min/\max,f}(\vec{r}_m; \vec{\xi})$, $XPD_{\min,f}(\vec{r}_m; \vec{\xi})$ and $XPI_f(\vec{r}_m; \vec{\xi})$ are the current parameters generated by the reflectarray; $\vec{\xi} = (\xi_1, \xi_2, \dots, \xi_{N \cdot N_{\text{DoF}}})$ is the vector of optimizing variables, which depends on the number of reflectarray elements (N) and the number of selected DoF that are optimized (N_{DoF}); and $W_{f,i}$, $i = 1, 2, 3$ is a weighting function that depends on the frequency and observation point. The weighting function is employed to balance the relative error in the optimized parameters among all coverage zones, polarizations and frequencies. It also allows to select which parameters are optimized. For instance, if $W_{f,1}(\vec{r}_m) \neq 0$, $W_{f,2}(\vec{r}_m) = W_{f,3}(\vec{r}_m) = 0$, a copolar only synthesis is carried out, since no cross-polarization parameters are considered in the cost function. Moreover, $W_{f,2}(\vec{r}_m)$ and $W_{f,3}(\vec{r}_m)$ allow to select only certain coverage zones and frequencies, allowing to optimize the XPD in the transmit band and the XPI in the receive band.

An in-house tool has been developed to implement the improved dual-band optimization algorithm.

C. Dual-Band Optimization Procedure

When considering all available DoF, there are more than 60 000 variables to be optimized. Taking into account the stringent requirements in Table I and that the gIA is a local-search algorithm, a brute-force optimization would not yield acceptable results. This is further challenged by the fact that extending the monochromatic case of previous works [15], [23] to a wideband, dual-band design does not result in a linear scaling in the problem, not only computationally, but also from the point of view of achieving the very stringent copolar and crosspolar requirements. In order to make convergence to a solution feasible, the dual-band optimization procedure will be divided in several stages. The result obtained at the end of each stage will be used as starting point on the following stage. In this way, convergence is improved since we reduce undesired local minima by gradually increasing the complexity of the problem and the total number of DoFs [24]. In addition, if a certain stage has led to an undesired local minimum, it can be modified without repeating previous stages. The dual-band optimization procedure is summarized in the flowchart of Fig. 3. A total of five stages are proposed in which the number of DoFs and difficulty of the problem are gradually increased.

1) *Stage 1*: The goal of the first stage is to obtain a reflectarray layout that fulfils requirements at a single frequency. This is done with a phase-only synthesis (POS) in dual-linear polarization and a zero-finding routine to adjust the size of the reflectarray elements. The procedure is detailed in [23]. The initial design will be carried out at the central frequency of the transmit band, $f_0 = 11.95$ GHz.

2) *Stage 2*: The second stage involves a dual-band optimization at six different frequencies, three in each band (central and extreme frequencies). In order to accelerate convergence and reduce the number of local minima, it will be a copolar-only synthesis using two DoFs per element, T_x and T_y , which are defined as $L_{a4} = T_x$, $L_{b1} = L_{b3} = 0.63T_x$, $L_{b2} = 0.93T_x$, $L_{b4} = 0.95T_y$, $L_{a1} = L_{a3} = 0.58T_y$, $L_{a2} = T_y$ (see Fig. 2). Thus, the weighting

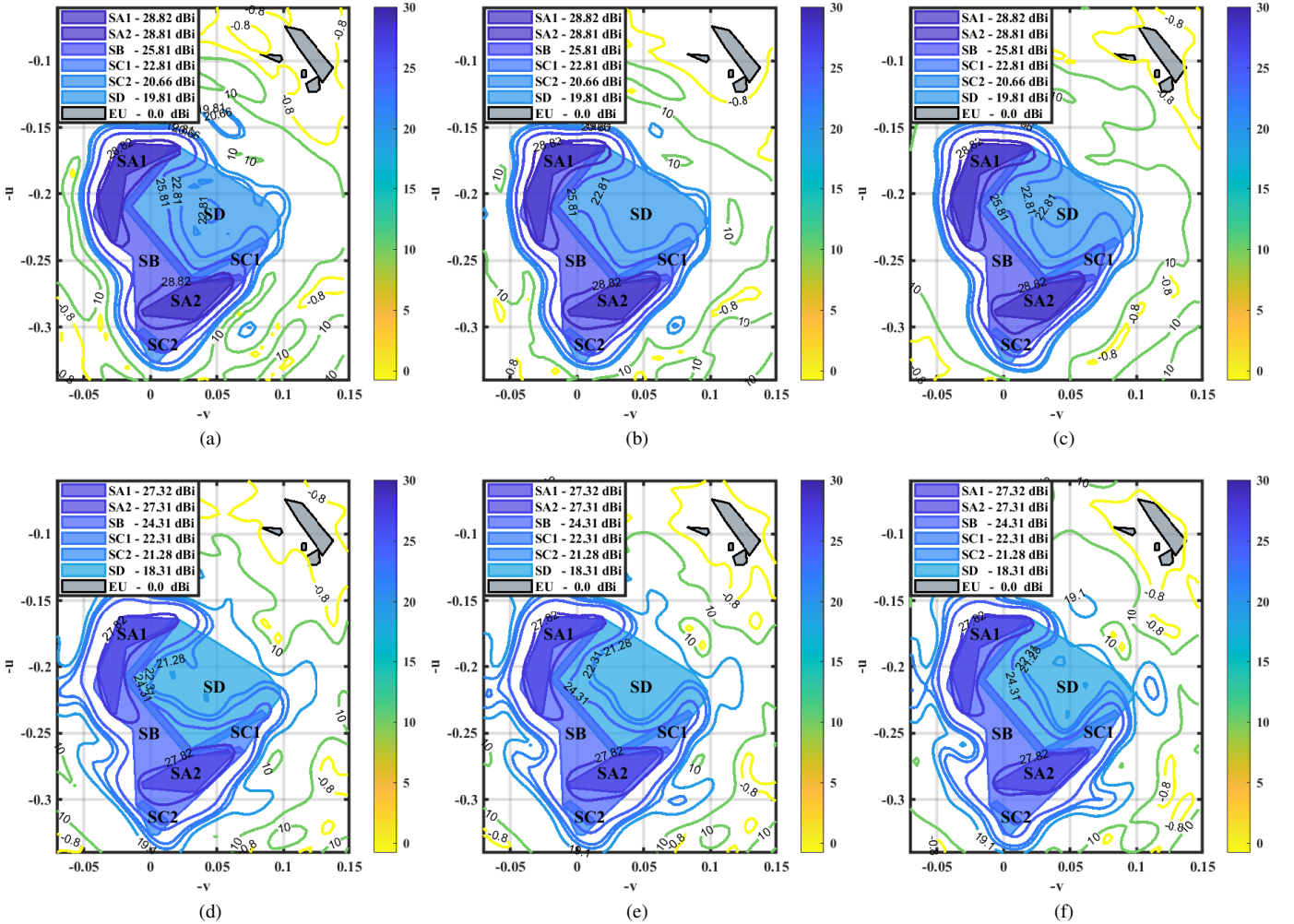


Fig. 4. For polarization Y, copolar component of the radiation pattern at (a) 11.70 GHz, (b) 11.95 GHz, (c) 12.20 GHz, (d) 13.75 GHz, (e) 14.00 GHz and (f) 14.25 GHz for the optimized reflectarray with South American coverage.

functions in (3) will satisfy:

$$W_{f,2}(\vec{r}_m) = W_{f,3}(\vec{r}_m) = 0. \quad (4)$$

Due to the large differences in gain of each zone, the weighting function $W_{f,1}(\vec{r}_m)$ will be used to balance the error of each coverage zone for each frequency and polarization.

3) *Stage 3*: The goal of the third stage is to further improve the copolar performance in both frequency bands by increasing the number of DoF from two to six, maintaining the cell symmetry. The DoFs are the lengths of all dipoles but maintaining the cell symmetry with $L_{a1} = L_{a3}$ and $L_{b1} = L_{b3}$.

4) *Stage 4*: The three previous stages have focused solely on minimum copolar requirements. However, by increasing the gain in each coverage zone, the cross-polarization performance is indirectly improved. Nonetheless, in practice this is not enough since copolar requirements may be met but not the cross-polarization ones. Thus, in this stage the XPD_{\min} and the XPI will be optimized, the XPD_{\min} in the transmit band and the XPI in the receive band (see Table I). This is done by setting the values of $W_{f,2}(\vec{r}_m)$ and $W_{f,3}(\vec{r}_m)$ in (3) to one at the appropriate frequency bands. The EU zone is also included now, minimizing its maximum copolar gain. In addition, the number of DoF per reflectarray element is maintained in six.

5) *Stage 5*: The copolar and cross-polarization requirements are kept and the number of DoF is increased to eight, breaking the cell

Table II
LOSS BUDGET IN dB FOR THE OPTIMIZED REFLECTARRAY.

Zone	T_x : 11.70 GHz – 12.20 GHz	R_x : 13.75 GHz – 14.25 GHz
SA1	0.62	0.88
SA2	0.69	0.88
SB	0.62	0.74
SC1	0.83	1.95
SC2	1.80	1.78
SD	0.78	0.73

symmetry. The goal is to refine the results obtained previously.

This procedure is general and can be applied with any kind of restrictions depending on the design goals. Limitations will be dictated by the physics of the problem, e.g., gain limited by the antenna size. It is also worth mentioning that this multi-objective and multi-stage design procedure is different from the ones employed in other works, and in particular in [17]–[19].

IV. RESULTS

After the POS and design at central frequency of stage 1, the simulated radiation patterns comply with specifications in both linear polarizations with at least 0.3 dB of loss budget, but only at

Table III
RESULTS OBTAINED FOR THE COPOLAR GAIN AND CROSS-POLARIZATION PERFORMANCE FOR THE REFLECTARRAY WITH SOUTH AMERICAN COVERAGE. GAIN REFERS TO MINIMUM COPOLAR GAIN WITH THE EXCEPTION OF EU, WHICH IS MAXIMUM COPOLAR GAIN.

Zone	T_x : 11.70 GHz – 12.20 GHz				R_x : 13.75 GHz – 14.25 GHz			
	Spec. Gain (dBi)	Gain (dBi)	Spec. XPD _{min} (dB)	XPD _{min} (dB)	Spec. Gain (dBi)	Gain (dBi)	Spec. XPI (dB)	XPI _{min} (dB)
SA1	28.82	29.44	31.00	35.22	27.32	28.20	32.00	38.62
SA2	28.81	29.50	31.00	37.05	27.31	28.19	28.00	39.78
SB	25.81	26.43	30.00	32.93	24.31	25.05	28.00	33.72
SC1	22.81	23.64	29.00	32.01	22.31	24.26	28.00	36.04
SC2	20.66	22.46	27.00	40.06	21.28	23.06	28.00	39.98
SD	19.81	20.59	27.00	28.23	18.31	19.04	25.00	28.28
EU	0.00	-0.88	—	—	0.00	-3.17	—	—

Table IV
REFLECTARRAY PERFORMANCE FOR POLARIZATION X AT 11.70 GHz. GAIN REFERS TO MINIMUM COPOLAR GAIN WITH THE EXCEPTION OF EU, WHICH IS MAXIMUM COPOLAR GAIN.

Zone	Gain (here)	Gain [19]	Gain [17]	XPD _{min} (here)	XPD _{min} [19]	XPD _{min} [17]
SA1	29.57	29.20	29.52	41.42	37.10	33.84
SA2	29.53	29.20	29.52	37.75	36.70	32.12
SB	26.51	26.20	26.10	36.60	35.40	30.35
SC1	23.79	23.20	23.18	32.87	34.10	27.74
SC2	22.97	21.10	25.34	40.06	32.00	35.35
SD	20.64	20.20	20.37	30.85	32.40	24.83
EU	-2.42	-0.40	-1.00	—	—	—

Table V
REFLECTARRAY PERFORMANCE FOR POLARIZATION X AT 14.25 GHz. GAIN REFERS TO MINIMUM COPOLAR GAIN WITH THE EXCEPTION OF EU, WHICH IS MAXIMUM COPOLAR GAIN.

Zone	Gain (here)	Gain [19]	Gain [17]	XPI (here)	XPI [19]	XPI [17]
SA1	28.31	27.70	27.79	40.49	34.00	26.82
SA2	28.29	27.70	27.52	41.55	34.80	33.56
SB	25.28	24.80	23.70	37.47	32.40	22.83
SC1	24.96	22.70	23.35	40.54	33.10	25.28
SC2	24.08	21.70	21.50	41.22	29.60	31.28
SD	19.97	18.80	17.16	31.23	26.40	18.18
EU	-6.87	-0.40	5.00	—	—	—

11.95 GHz. Other frequencies at the transmit and receive bands do not comply at all, although the transmit band presents better results than the receive band. Even though stages 2 and 3 focus only on optimizing the copolar pattern, the cross-polarization performance is improved indirectly due to the definitions of the XPD_{min} and XPI parameters. In stage four, cross-polarization requirements were added, but the CP_{min} is favoured in the optimization since it is the critical parameter due to the size of the antenna. As a result, the cross-polarization improves moderately while the coverage zones comply with all copolar requirements with at least 0.38 dB of budget loss. Finally, in the last stage the number of DoF is increased to eight to increase the loss budget to 0.62 dB. In this final stage, the optimization was carried out with a total of 61 380 DoFs.

The final optimized reflectarray complies with all the coverage requirements in both linear polarizations and frequency bands for both minimum copolar gain and cross-polarization performance. The worst results are obtained for Y polarization, whose copolar radiation patterns are shown in Fig. 4 for the six frequencies considered in the optimization. In fact, all requirements are met with a loss budget of at least 0.62 dB. This minimum loss budget is produced in SA1 at 11.70 GHz and SB at 12.20 GHz, both for polarization Y. Table II shows the loss budget per coverage zone for both bands. The loss budget takes into account the different gain requirements of Table I, which along the fact that in the upper band the antenna is electrically larger, it explains the differences in loss budget between both bands.

The worst results at each band are summarized in Table III, including both copolar and cross-polarization requirements. One important feature of the present design is that it achieves better results than the antenna presented in [19], with the exception of the worst XPD_{min} for SA1, SB, SC1 and SD, and the XPI in SB, in polarization Y. Nevertheless, the design presented here also complies with all requirements, while achieving a loss budget of 0.62 dB, while in [19] the loss budget is 0.40 dB. In addition, the

achieved isolation for Europe is at least -0.88 dB while in [19] is -0.40 dB. Moreover, the reflectarray in [19] is circular with a diameter of 1.2 meters and employs an ideal far field model for the feed horn, while the antenna designed here is smaller, having two main axes of 1.10 and 1.08 meters, and considers the near field of a real corrugated feed horn. This supposes a 17% reduction of the aperture size (considering the ellipse surface), reducing also the weight. Overall, a better performance is therefore achieved, including better minimum copolar gain and isolation, while using an antenna with a smaller size. It also achieves better results than the designs presented in [17] and [18], where the diameter of the antennas were 1.2 and 1.1 meters, respectively. Tables IV and V compare the results for polarization X at 11.70 GHz and 14.25 GHz with those reported in [17] and [19]. Polarization X corresponds to the vertical polarization (V) in [17], [19] due to the orientation of the antenna, where the horizontal polarization is defined with the electric field parallel to the equatorial plane [18].

Fig. 5 shows the contours for the XPD at 11.70 GHz for polarization Y. This frequency and polarization represents the worst case of cross-polarization performance of the optimized reflectarray, but still complies with requirements, as shown in Table III. Finally, Table VI presents a summary of the computational performance of the algorithm for each stage, including total memory usage. The overall time taken by the optimization procedure was almost 6.5 days.

V. CONCLUSIONS

In this work, a novel dual-band design procedure based on a multi-resonant unit cell with several degrees of freedom has been presented. It is divided in several stages to facilitate convergence towards a dual-band high-performance design. First, a phase-only synthesis (POS) is carried out at central frequency, obtaining a narrowband design. Then, a broadband copolar-only optimization is performed using a limited number of degrees of freedom. In this

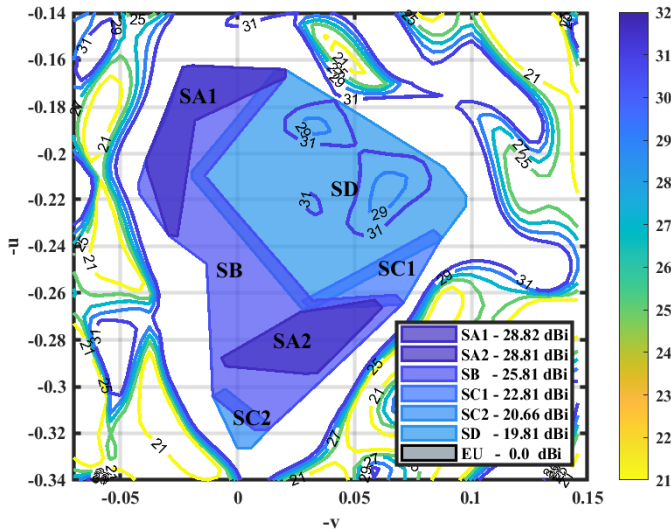


Fig. 5. Crosspolar discrimination (XPD) contours in dB at 11.70 GHz for polarization Y. This case presents the worst cross-polarization performance, with a XPD_{\min} for zone SD of 28.23 dB.

Table VI

COMPUTATIONAL PERFORMANCE OF THE ALGORITHM FOR THE FIVE STAGES IN A WORKSTATION WITH TWO INTEL XEON E5-2650V3.

Stage	# variables	Time per iteration	# iterations	Memory
1	7772	14.7 s	261	0.8 GB
2	15345	492.6 s	91	1.78 GB
3	46035	1423.5 s	116	15.9 GB
4	46035	1423.5 s	113	15.9 GB
5	61380	2145.9 s	86	28.2 GB

stage, only copolar requirements are imposed, greatly improving the broadband performance of the reflectarray antenna. Finally, the cross-polarization performance is also optimized, but now using more degrees of freedom. This design procedure has been applied to a very large, transmit-receive reflectarray for direct broadcast satellite application with improved copolar and cross-polarization performances. The reflectarray provides coverage for the PAN_S mission of the Amazonas satellite in transmit and receive bands, and in dual-linear polarization. The optimized reflectarray complies with all requirements with a loss budget of 0.62 dB. The performance of the reflectarray antenna designed in this work is better than other designs reported in the literature while using a smaller aperture size and the near field of a real feed horn. The direct optimization procedure proposed here demonstrates the capability of reflectarray antennas to provide service for space applications in a large bandwidth with stringent co- and cross-polarization requirements.

REFERENCES

- [1] J. Huang and J. A. Encinar, *Reflectarray Antennas*. Hoboken, NJ, USA: John Wiley & Sons, 2008.
- [2] R. Florencio, J. A. Encinar, R. R. Boix, V. Losada, and G. Toso, "Reflectarray antennas for dual polarization and broadband telecom satellite applications," *IEEE Trans. Antennas Propag.*, vol. 63, no. 4, pp. 1234–1246, Apr. 2015.
- [3] V. Richard, R. Loison, R. Gillard, H. Legay, M. Romier, J.-P. Martinaud, D. Bresciani, and F. Delepaux, "Spherical mapping of the second-order phoenix cell for unbounded direct reflectarray copolar optimization," *Progr. Electromagn. Res. C*, vol. 90, pp. 109–124, 2019.
- [4] L. Guo, P.-K. Tan, and T.-H. Chio, "On the use of single-layered subwavelength rectangular patch elements for broadband folded reflectarrays," *IEEE Antennas Wireless Propag. Lett.*, vol. 16, pp. 424–427, 2017.
- [5] R. S. Malfajani and Z. Atlasbaf, "Design and implementation of a broadband single-layer reflectarray antenna with large-range linear phase elements," *IEEE Antennas Wireless Propag. Lett.*, vol. 11, pp. 1442–1445, 2012.
- [6] P.-Y. Qin, Y. J. Guo, and A. R. Weily, "Broadband reflectarray antenna using subwavelength elements based on double square meander-line rings," *IEEE Trans. Antennas Propag.*, vol. 64, no. 1, pp. 378–383, Jan. 2016.
- [7] M. Zhou, S. B. Sørensen, O. Borries, and E. Jørgensen, "Analysis and optimization of a curved transmit-receive contoured beam reflectarray," in *The 9th European Conference on Antennas and Propagation (EuCAP)*, Lisbon, Portugal, Apr. 13–17, 2015, pp. 1–5.
- [8] H. Legay, D. Bresciani, E. Labiole, R. Chiniard, and R. Gillard, "A multi facets composite panel reflectarray antenna for a space contoured beam antenna in Ku band," *Progr. Electromagn. Res. B*, vol. 54, pp. 1–26, Aug. 2013.
- [9] H. Hasani, M. Kamyab, and M. Ali, "Low cross-polarization reflectarray antenna," *IEEE Trans. Antennas Propag.*, vol. 59, no. 5, pp. 1752–1756, May 2011.
- [10] C. Tienda, J. A. Encinar, M. Arrebola, M. Barba, and E. Carrasco, "Design, manufacturing and test of a dual-reflectarray antenna with improved bandwidth and reduced cross-polarization," *IEEE Trans. Antennas Propag.*, vol. 61, no. 3, pp. 1180–1190, Mar. 2013.
- [11] R. Florencio, J. A. Encinar, R. R. Boix, G. Pérez-Palomino, and G. Toso, "Cross-polar reduction in reflectarray antennas by means of element rotation," in *10th European Conference on Antennas and Propagation (EuCAP)*, Davos, Switzerland, Apr. 10–15, 2016, pp. 1–5.
- [12] S. Mercader-Pellicer, G. Goussetis, G. M. Medero, D. Bresciani, H. Legay, and N. J. G. Fonseca, "Cross-polarization reduction of linear-to-circular polarizing reflective surfaces," *IEEE Antennas Wireless Propag. Lett.*, vol. 18, no. 7, pp. 1527–1531, Jul. 2019.
- [13] M. Zhou, S. B. Sørensen, O. S. Kim, E. Jørgensen, P. Meincke, and O. Breinbjerg, "Direct optimization of printed reflectarrays for contoured beam satellite antenna applications," *IEEE Trans. Antennas Propag.*, vol. 61, no. 4, pp. 1995–2004, Apr. 2013.
- [14] M. Zhou, S. B. Sørensen, O. S. Kim, E. Jørgensen, P. Meincke, O. Breinbjerg, and G. Toso, "The generalized direct optimization technique for printed reflectarrays," *IEEE Trans. Antennas Propag.*, vol. 62, no. 4, pp. 1690–1700, Apr. 2014.
- [15] D. R. Prado, M. Arrebola, M. R. Pino, R. Florencio, R. R. Boix, J. A. Encinar, and F. Las-Heras, "Efficient crosspolar optimization of shaped-beam dual-polarized reflectarrays using full-wave analysis for the antenna element characterization," *IEEE Trans. Antennas Propag.*, vol. 65, no. 2, pp. 623–635, Feb. 2017.
- [16] D. R. Prado, J. A. López-Fernández, M. Arrebola, and G. Goussetis, "Support vector regression to accelerate design and crosspolar optimization of shaped-beam reflectarray antennas for space applications," *IEEE Trans. Antennas Propag.*, vol. 67, pp. 1659–1668, Mar. 2019.
- [17] J. A. Encinar, M. Arrebola, L. F. de la Fuente, and G. Toso, "A transmit-receive reflectarray antenna for direct broadcast satellite applications," *IEEE Trans. Antennas Propag.*, vol. 59, no. 9, pp. 3255–3264, Sep. 2011.
- [18] J. A. Encinar, R. Florencio, M. Arrebola, M. A. Salas-Natera, M. Barba, J. E. Page, R. R. Boix, and G. Toso, "Dual-polarization reflectarray in Ku-band based on two layers of dipole arrays for a transmit-receive satellite antenna with South American coverage," *Int. J. Microw. Wirel. Technol.*, vol. 10, no. 2, pp. 149–159, 2018.
- [19] M. Zhou, O. Borries, and E. Jørgensen, "Design and optimization of a single-layer planar transmit-receive contoured beam reflectarray with enhanced performance," *IEEE Trans. Antennas Propag.*, vol. 63, no. 4, pp. 1247–1254, Apr. 2015.
- [20] "GRASP v10," TICRA, Copenhagen, Denmark.
- [21] D. R. Prado and M. Arrebola, "Effective XPD and XPI optimization in reflectarrays for satellite missions," *IEEE Antennas Wireless Propag. Lett.*, vol. 17, no. 10, pp. 1856–1860, Oct. 2018.
- [22] R. Florencio, R. R. Boix, and J. A. Encinar, "Enhanced MoM analysis of the scattering by periodic strip gratings in multilayered substrates," *IEEE Trans. Antennas Propag.*, vol. 61, no. 10, pp. 5088–5099, Oct. 2013.
- [23] D. R. Prado, J. A. López-Fernández, M. Arrebola, M. R. Pino, and G. Goussetis, "General framework for the efficient optimization of reflectarray antennas for contoured beam space applications," *IEEE Access*, vol. 6, pp. 72 295–72 310, 2018.
- [24] O. M. Bucci, G. D'Elia, G. Mazzarella, and G. Panariello, "Antenna pattern synthesis: a new general approach," *Proc. IEEE*, vol. 82, no. 3, pp. 358–371, Mar. 1994.